INSTITUTE OF PHYSICS PUBLISHING JOURNAL OF PHYSICS D: APPLIED PHYSICS

J. Phys. D: Appl. Phys. **36** (2003) 2487–2497 PII: S0022-3727(03)62289-8

Theoretical analysis of electrical transient behaviour in TEA CO_2 laser with dielectric corona pre-ionization

Alireza Bahrampour[1,2] **and Alireza A Ganjovi**[2]

[1] Valie Asr university, Rafsanjan, Iran
[2] International Center for Science & High Technology & Environmental Science (ICST), Kerman, Iran

E-mail: alirezaganjovi@yahoo.com

Received 13 April 2003
Published 1 October 2003
Online at stacks.iop.org/JPhysD/36/2487

Abstract
In this paper a theoretical model for transient behaviour analysis of the discharge current pulse in the transversely excited atmospheric pressure CO_2 laser with dielectric corona pre-ionization is presented. The laser discharge tube is modelled by a non-linear distributed RLC electric circuit. The transmission line method is applied to the non-linear distributed circuit and it is approximated by a lumped non-linear RLC circuit. By this method the governing partial differential equations are reduced to a system of ordinary differential equations. The governing ordinary differential equations of the lumped non-linear RC electric circuit are solved numerically. On the basis of this model the pre-ionization and main discharge energies are evaluated. Our theoretical results are in good agreement with the published experimental observations.

1. Introduction

After the discovery of the transversely excited atmospheric pressure (TEA) CO_2 laser by Dumanchin [1] and Beaulieu several ultraviolet (UV) [2–7] and electron beam (EB) [8–10] pre-ionization techniques have been developed. Experiments have also indicated that uniform pre-ionization is highly desirable. So it is very important that the UV source be uniform and extends over an area equal to the length of the electrodes times their separation distance. The most successful technique for achieving this is the use of a dielectric corona discharge, which was pioneered by Ernst and Boer [11–14]. For nearly all other UV pre-ionization laser systems, theoretical and experimental investigations have been carried out by previous investigators [2–7]; the electric equivalent models are ordinary electric circuit [15, 16] and can be analysed by commercial electric circuit analysis packages [17].

In dielectric corona discharge techniques, the UV pre-ionization is different from other UV pre-ionizations by the fact that no additional UV source is present, the UV source is uniformly and continuously distributed along the laser tube and the excitation rate is very fast.

The mechanism of the corona pre-ionization is reflected in the laser current pulse waveform. The electric equivalent circuit of the TEA CO_2 laser with dielectric corona pre-ionization is a non-linear distributed RC circuit that is presented in this paper and analysed by the transmission line method (TLM) [18]. The method is applied to numerical analysis of the transient behaviour of the TEA CO_2 laser with dielectric corona pre-ionization. The numerical results are in good agreement with the previous experimental data, which are published by Ernst and his colleagues [12]. The theory is also applied in order to determine the variation of the radiated UV intensity with respect to variation of the geometrical and physical parameters of the dielectric.

In section 2 of this paper the structure of the laser tube and its equivalent circuit are described; on the basis of the formula of Morrow and Sato the parameters of the equivalent circuit are evaluated. The current and voltage propagation on the dielectric plates are given by the TLM in section 3 of this paper. In this section, the continuity equations for the main discharge region and the regions near the dielectric plates, with the related photo-ionization, sources are also discussed. Since the continuity equations are of ordinary type and the transmission line equations are partial differential equations, instead of the

solution of the partial differential equation in section 4, the transmission line is approximated by a lumped RLC network, and the partial differential equations are approximated by a system of ordinary differential equations. Then by the solution of this system of ordinary differential equations the transient behaviour of the anode current of the laser tube is obtained. In sections 5 and 6 the results of the calculations and conclusions are presented, respectively.

2. Laser tube structure and its equivalent circuit

For a homogeneous self-sustained discharge in the TEA laser tube an initial distribution of free electrons within the discharge volume would be required. Such an initial distribution of free electrons or pre-ionization can be provided by any suitable volume ionization source such as UV light, x-ray and γ-ray, particle and electron beams, etc [19].

When a dielectric plate is subjected to a high electric voltage, the field polarizes the dielectric plate and a high field is presented at its surface. The high electric field produces a partial breakdown or corona discharge in the surrounding gas near the dielectric.

This mechanism has been applied to several different laser structures. Ernst and Boer use two suitable dielectric sheets parallel to the optical axis and perpendicular to the electrodes, as shown in figure 1(*b*), through an electric circuit (a Marx bank generator), as shown in figure 1(*a*); a high voltage pulse is suddenly applied to the electrodes of this structure. Since the cathode has a metallic extension bent around the two dielectric plates and closely approaching the anode, the dielectric plates are subjected to a very strong electric field. They become polarized with surface charges as shown in figure 1(*b*). The strong electric field in the surrounding gas produces a surface corona discharge. The electrons are accelerated in the strong electric field and the ions formed in the surrounding gas are attracted by the dielectric plates. The electrons are easily pulled out from the gas layer via the strong electric field in the corner formed by the dielectric and the anode. Once sufficient electrons are present in the gas layers, streamers are formed and rapidly develop into avalanches [20]. Because of the non-conductivity of the dielectric, the surface discharge is uniform in the direction of the optical axis, i.e. perpendicular to figure 1(*b*). The plasma produced near the dielectric plates forms a channel with a width equal to the length of the electrodes for passage of current from the anode to the cathode. The corona surface current emits UV photons [21].

The UV photons emitted by this uniform dielectric corona discharge illuminate the cathode gap uniformly in the direction of the optical axis. This is not necessarily the case in the direction across the width of the plate. A gradient in the direction of the current does not influence the quality of the resulting main discharge [8]. A major uniformity of glow discharge in the main discharge region is given by the pre-ionization density. In this vein, Levatter and Lin modelled the early stages of development of high pressure pre-ionized pulsed gas discharges [22]. Using the Levatter and Lin criterion, microscopically uniform CO_2 laser discharges can only be obtained if the initial pre-ionization electron density $(n_e)_0$ is:

$$(n_e)_0 \geqslant \left(\frac{5\times 10^6}{t_0^{2/3}}\right) p^{3/2},$$

where t_0 is the voltage rise time (ns) and p is the gas pressure (atm). For typical discharges ($t_0 = 100$ ns, $p = 1$ atm) one must have $(n_e)_0 \geqslant 10^5\,\mathrm{cm}^{-3}$. This is a value that is easily obtained in TEA CO_2 laser discharges using dielectric corona pre-ionization [23].

Electrically, the gas discharge in the laser channel constitutes an element of the entire electric circuit of the laser system and this represents a time dependent and non-linear RLC electric circuit. The study of the laser tube structure can be divided into two separate parts, the main discharge region and the pre-ionization section. Persephonise *et al* have modelled the main discharge section of the pulsed gas-laser tube by a time dependent resistor and an inductor in series combination [24–28], They have assumed that in the inter-electrode space of the gas laser chamber, a strong source of pre-ionization provides the initial electron number density, which is sufficiently higher than the minimum necessary pre-ionization density for a homogeneous glow discharge.

In this work we use the Morrow and Sato formula [29, 30] for the current flowing in an external circuit due to the motion

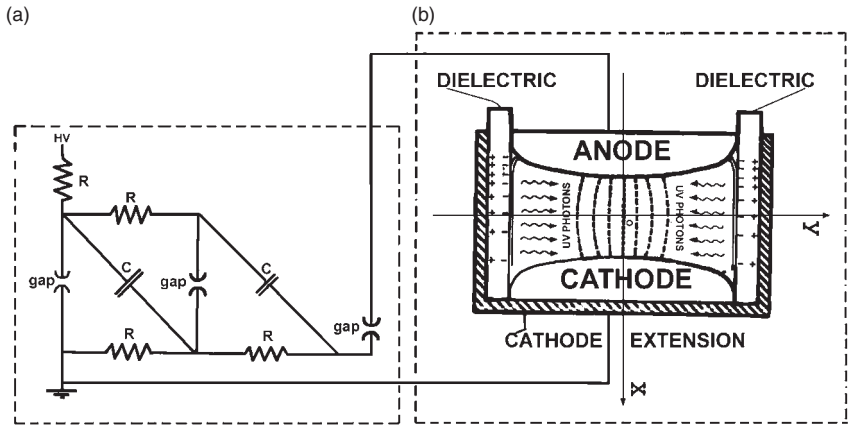

Figure 1. A schematic of a TEA CO_2 laser system with dielectric corona pre-ionization: (*a*) electrical system of the laser system, (*b*) a cross section perpendicular to the optical axis of the laser tube.

of charged particles in a gas with a time dependent external applied voltage:

$$I = \left(\frac{e}{V_A}\right)\int_V (n_p V_p - n_e V_e - n_n V_n - D_p \nabla n_p + D_e \nabla n_e + D_n \nabla n_n) \cdot E_0 \, dV + \left(\frac{\varepsilon_0}{V_A}\right)\int_V \frac{\partial E_0}{\partial t} \cdot E_0 \, dV, \quad (1)$$

where n_e, n_p, and n_n are the electron density, the positive ion density and the negative ion density, respectively, V_e, V_p and V_n are the electron, positive ion and negative ion velocity vectors, respectively, D_e, D_p and D_n are the electron , positive ion and negative ion diffusion coefficients, respectively, and E_0 is the electric field vector due to the external voltage, V_A, and it is a solution of the Laplace equation:

$$\nabla \cdot E_0 = 0. \quad (2)$$

On the timescale of interest in a typical short duration pulsed discharge, the electrons are free to move towards the anode while the ions are essentially frozen in space; furthermore, since the diffusion coefficient relative to the mobility coefficient in high pressure gases is very low [8], the pre-ionization process makes the diffusion of charged particles nearly uniform in the space discharge region [22] and the electron and ion diffusion times are much larger than the applied voltage pulse width time [31], the diffusion and ion current densities are negligible with respect to the electron drift current density [32]. Hence Morrow and Sato's formula can be rewritten as follows:

$$I = -\left(\frac{e}{V_A}\right)\int_V n_e V_e \cdot E_0 \, dV + \left(\frac{\varepsilon_0}{V_A}\right)\int_V \frac{\partial E_0}{\partial t} \cdot E_0 \, dV. \quad (3)$$

For a laser tube with maximally uniform electric field electrodes, such as Ernst, Rogrowsky and Chang types, the electric field is nearly constant in the main discharge region ($E_0 = V_A/d$) and the electron drift velocity is:

$$V_e = \mu_e(E_0 + E'), \quad (4)$$

where μ_e is the electron mobility and E' is the electric field due to the space-charge in the main discharge region. It is noted that E' is a solution of the Poisson equation:

$$\nabla \cdot E' = \frac{e}{\varepsilon_0}(n_p - n_e - n_n). \quad (5)$$

With the assumption that the electric field is uniform in the main discharge region ($V_A = E_0 d$), equation (3) can be rewritten in the following form:

$$I = gV_A + C_s \frac{\partial V_A}{\partial t}, \quad (6)$$

where C_s is the stray capacitance between the laser electrodes [33], V the discharge volume, S the electrode surface area and g is the conductance of the plasma in the discharge region:

$$g = \frac{e\mu_e S}{d}\frac{1}{V}\int_V n_e \left(1 + \frac{E'}{E_0}\right) dV, \quad (7)$$

where d is the separation distance between the laser electrodes. The electron number density, n_e, is time dependent and is a solution of the continuity equation. Equation (1) shows that the main discharge region of the laser tube is electrically the same as a parallel combination of a capacitor and a time dependent resistor. If the inductance of the laser tube is not neglected, then, as shown in figure 2, the main discharge region is equivalent to an electric circuit that consists of the stray capacitance parallel with a series combination of an inductor and a time dependent resistor (see figure 2(b)).

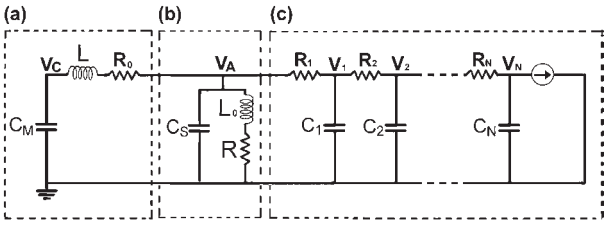

Figure 2. An electric equivalent circuit for a TEA CO_2 laser system with dielectric corona pre-ionization: (a) equivalent circuit of the driving circuit of the laser tube, (b) electric equivalent circuit of the main discharge part of the laser tube, (c) electric equivalent circuit of the pre-ionizer part of the laser tube. The resistance in (b) and all resistances in (c) coupled through the UV radiation emitted by resistances.

A transient gas discharge, such as a micro-discharge or dielectric barrier discharges, occurs at atmospheric pressure between electrodes where at least one electrode is covered with a barrier dielectric discharge. These discharges consist generally of a large number of short lived parallel filaments also called micro-discharges. Theoretical and experimental studies of the atmospheric pressure micro-discharges have been reported by previous investigators [34].

The pre-ionization part of the laser tube consists of the metallic extensions of the cathode, which are covered by the dielectric plates, and the anode of the laser tube. Electrically the pre-ionization part of the laser tube is equivalent to a distributed time dependent non-linear RC circuit in which each of the capacitances (C_j) consists of an infinitesimal portion of the dielectric plates and their back metallic extensions. The capacitances are charged through the micro-discharges. On the basis of equation (1) the micro-discharges electrically have the same behaviour as a time dependent non-linear resistance (R_j). In the distributed time dependent non-linear equivalent RC circuit, the secondary cathode photo-emission effect is considered as the boundary condition and in a lumped RC equivalent circuit, as shown in figure 2(c), it is represented by a current source I_S. Finally, the driving circuit of the laser system is represented by an RLC network, as shown in figure 2(a), where RLC is the representation of the ignition and transmission part of the system and C_M is the main energy storage capacitance of the laser system. The time dependent behaviour of the laser circuit is obtained from network analysis of figure 2.

3. Model simulation

A schematic representation of the equivalent electric circuit of the TEA CO_2 laser tube with dielectric corona pre-ionization is shown in figure 2. In order to determine the distribution of the discharge input energy that is transferred to various vibrational modes, excited electronic states, dissociation

ionization as well as transport coefficients, detail knowledge of the electronic density and its energy distribution function, $f(\varepsilon)$, are required. The most important transport coefficients determining macroscopic properties of the discharge are the electron drift velocity and ionization and attachment coefficients, which can be calculated as a function of (E/N_0). Lowke *et al* [35] have numerically calculated the electron distribution function for a variety of experimentally interesting electric discharge conditions using the measured cross sections for elastic and inelastic collisions. We have used their analysis with the presumption of spatial uniformity and steady state calculation. We can do this because the discharge operates at a high pressure and therefore the distribution of electron energies is practically always in equilibrium with the applied field. The time constant of the inherent changes in the electric field due to space-charges build up, and it is of the order of 10^{-9} s. On the other hand, the time it takes for the electrons to reach equilibrium at 1 atm is of the order of 10^{-11} s or less [31].

The basic assumptions of the model are as follows:

(1) The charged particles are in local equilibrium states for local electric fields. All transport coefficients, such as drift velocity, diffusion coefficients and ionization coefficients, are assumed to be dependent only on the local electric field over background gas density (E/N_0); with these assumptions, the electron and ion transport can be described by using the continuity equation instead of the Boltzmann equation [36, 37].
(2) The particle flux is described by the drift approximation where the effect of convective and diffusion gas flow is negligible. Convective and diffusion gas flow will not be an important factor when the gas diffusion time is much greater than the applied voltage pulse time width.
(3) Since ions are much heavier than electrons, ions cannot gain enough energy from the applied field and the ion currents are negligible.
(4) Negative ions are neglected.
(5) The inductance and stray capacitance of the main discharge region are neglected.

The continuity equation for electrons is:

$$\frac{\mathrm{d}n_{ei}(r,t)}{\mathrm{d}t} = S_i(r,t) + \alpha_i|V_{ei}|n_{ei}(r,t) - \beta n_{ei}^2(r,t), \quad i = \mathrm{M}, \mathrm{T}, \tag{8}$$

where β, α, V_e and $S_i(r,t)$ are the recombination rate coefficient, the ionization coefficient, the drift velocity of electrons and the rate of photo-ionization, respectively. The indices $i = \mathrm{M}, \mathrm{T}$ correspond to the main discharge region and the near dielectric plates region, respectively.

Near the dielectric plates, barrier discharges or micro-discharges are developed. In developing the streamer theory of gaseous breakdown, Loeb and Meek [38] took as a basis the fact that strong photo-ionization occurs in the vicinity of an avalanche, thus ensuring a continuous and adequate supply of new electrons that will create secondary avalanches [39]. The latter will be drawn into the space-charge channel, and it will in this way advance towards the anode. A detailed criticism of the Loeb–Meek theory is given in Firsov's dissertation [40, 41]. The photo-ionization source near the dielectric plates is written as follows:

$$S_{\mathrm{T}}(x,t) = A_{r0}\int K(|x-x'|)n_{\mathrm{e}}(x',t)\,\mathrm{d}x', \tag{9}$$

where A_{r0} is the transition probability for the resonance transition and $K(|x-x'|)$ is the law of absorption of the photo-ionizing radiation, which is a function of the absorption coefficient of the medium and the line form of the radiation. The law of absorption $K(|x-x'|)$ is determined by Lozanskii and Holstien for different absorption coefficients and line forms [42, 43]. In this work we have assumed that the absorption coefficient and line forms have a Lorentzian line shape. According to Lozanskii [44–47] calculations, the law of absorption can be shown in the following form:

$$K(|x-x'|) = \frac{1}{\sqrt{(4\pi)^3\kappa_0}|x-x'|^{7/2}}, \tag{10}$$

where κ_0 is the absorption coefficient of a central photon at the resonance frequency. Equation (9) is used in the continuity equation for the near dielectric plate regions.

The UV radiation emitted by the micro-discharges on the dielectric plates also propagated in the main discharge region. In this investigation we use the Beverly method [21, 48–51], where the rate of photo-ionization is given by

$$S_{\mathrm{M}}(y,t) = \int_{\lambda_1}^{\lambda_2}\sigma_t(\lambda)N_0\varphi(\lambda,y,t)\,\mathrm{d}\lambda, \tag{11}$$

where $\sigma_t(\lambda)$ is the photo-ionization cross section, φ is photon flux at a wavelength λ, nm, which reaches a distance $(b/2-y)$ and $(b/2+y)$ from the photon sources right and left dielectric plates, respectively, and is given by

$$\varphi(\lambda,y,t) = \left(\frac{\lambda P(\lambda,t)}{hc}\right)\cdot\left\{\exp\left[-\sigma_{\mathrm{a}}(\lambda)N_0\left(\frac{b}{2}-y\right)\right] + \exp\left[-\sigma_{\mathrm{a}}(\lambda)N_0\left(\frac{b}{2}+y\right)\right]\right\}, \tag{12}$$

where h, $\sigma_{\mathrm{a}}(\lambda)$ and c are the Plank constant, the total absorption cross section and the light velocity. b is the distance between the dielectric plates and $P(\lambda,t)$ is the spectral irradiance [21]. We are assuming that it is proportional to the instantaneous wasted power in the surface resistance, $R(x,t)$:

$$P(\lambda,t) = \eta(\lambda)\int_{-d/2}^{d/2}R(x,t)\,i^2(x,t)\,\mathrm{d}x, \tag{13}$$

where $R(x,t)$ and $i(x,t)$ are the resistance of the plasma layer on the dielectric per unit width and the current at an instant t and at a point on the dielectric plate that is at a distance x from the anode. $\eta(\lambda)$ is a spectral characteristic of the radiation source and is determined by the experimental results [5]. The spectral irradiance is strongly related to (i) the mixture of the gas environment, (ii) the magnitude and rate of energy deposition into the corona discharge region and (iii) a weaker dependence, the gas pressure.

In the corona discharge region, the effects of the electrode substance and dielectric composition on the spectral irradiance are negligible, and the UV spectrum of the emitted light is strongly determined by the mixture of the environment. Our calculations are based on the experimental results of Seguin *et al* [4, 52] and Babcock *et al* [5], which are also in agreement with the data used by Ernst and his colleagues [11–14].

A vast amount of data exist for the absorption of CO_2, N_2 and He in the 115–200 nm regions [8, 52]. There is no appreciable absorption in these gases at wavelengths greater

than 200 nm, and laser gases containing about 0.1 atm of CO_2 are essentially black for wavelengths shorter than 115 nm. Experimental observations show that nitrogen gas is the primary source of hard UV photons in dielectric surface discharge. This intense and relatively broad emission from nitrogen is rapidly attenuated and filtered by the CO_2 molecules present in the laser mixture such that only two useful bands remain, one ∼5 nm wide centred at 120 nm and another about 10 nm wide centred near 175 nm. The photo-ionization obtained in the laser mixture is found to correlate well with these two narrow transmission bands [4, 5, 8]. In each of the above bands, there are many narrowband emissions. The envelope of the spectrum of the filtered emission is normalized to the total radiation energy emitted by the nitrogen molecule on the surface of the dielectric and it is denoted by $f_s(\lambda)$. This function is approximated by two Lorentzian lines centred at 120 nm (λ_A) and 175 nm (λ_B) and being 5 nm ($\Delta\lambda_A$) and 10 nm ($\Delta\lambda_B$) wide, respectively:

$$f_s(\lambda) = \frac{2A/(\pi\,\Delta\lambda_A)}{1+4((\lambda-\lambda_A)/\Delta\lambda_A)^2} + \frac{2B/(\pi\,\Delta\lambda_B)}{1+4((\lambda-\lambda_B)/\Delta\lambda_B)^2}\ (\mathrm{nm}^{-1}), \tag{14}$$

where the constants A and B are obtained from experimental results [52] and are presented in table 2. The spectral characteristic of the radiation is given by

$$\eta(\lambda) = \zeta\ f_s(\lambda), \tag{15}$$

where ζ is the electrical energy to radiation energy conversion efficiency [53].

Previous theoretical and experimental research have shown that the electric field distribution, as influenced by the electrode profiles and the uniformity of the photo-electron density in planes parallel to the main discharge electrodes, plays an important role in UV recognized self-sustained glow discharges in CO_2 laser gas mixtures [8]. Their parameters affect the homogeneity of the glow discharge and hence the maximum energy loading into the discharge volume. It is also shown that there is a threshold density of initial photo-electrons for formation of a uniform glow for each specified set of discharge parameters. Increasing the energy supplied to the pre-ionization source has minimal impact on the discharge [21]. Estimates of this pre-ionization threshold density, however, show that this must be some orders of magnitude greater than that attributed to natural background radiation, typically 10^9–10^{11} cm^{-3} [22], compared with a background of 10^2 cm^{-3} [54]. In this analysis we have assumed that there exist all the necessary conditions for the existence of uniform and homogeneous self-sustained glow discharge in the active medium of the TEA CO_2 laser [22]. The photo-ionization rate given by equation (11) is used in the continuity equation for the main discharge region.

Let the distance between two adjacent electric nodes in the circuit of figure 2(*c*) be an infinitesimal (dx); then the Kirchhoff current and voltage laws are written as follows:

$$\frac{\partial V(x,t)}{\partial x} = i(x,t)R(x,t), \tag{16}$$

$$\frac{\partial V(x,t)}{\partial t} = \frac{i(x,t)}{C(x,t)}, \tag{17}$$

where $V(x,t)$ is the voltage at instant t and at a point on the dielectric plate that is at a distance x from the anode electrode and $C(x,t)$ is the capacitance constructed between the plasma layer and metallic extension bent around the two dielectric plates per unit width. The capacitance per unit width is:

$$C = k\varepsilon_0\left(\frac{l}{w}\right), \tag{18}$$

where k, l and w are dielectric relative permittivity, laser length and dielectric thickness, respectively. The resistance per unit width of the plasma column is from equation (7). For a homogeneous self-sustained gas discharge, the conductance between the laser electrodes in the main discharge region ($g(t) = 1/R(t)$) can be approximated by a parallel combination of some conducting strips.

The continuity and transmission line equations are coupled through the electron density dependence of the resistance of each of the regions and the electric field dependence of the Townsend ionization coefficients [8].

The boundary conditions for the electronic current on the cathode and external applied voltage on the anode are given by Morrow [30]:

$$V\left(\frac{-d}{2},t\right) = V_A(t),$$

$$I_c\left(\frac{d}{2},t\right) = \frac{1}{\tau}\int_0^t \exp\left(-\frac{t-t'}{\tau}\right) \times \int_{-d/2}^{d/2} \gamma_p\delta(x,t')I_c(x,t')\cdot\exp(-\mu x)\,\mathrm{d}x\,\mathrm{d}t', \tag{19}$$

where γ_p is the secondary electron emission coefficient due to photon impact and the excited state, μ is the absorption coefficient, τ is the lifetime and $\delta(E/N_0)$ is the electron excitation coefficient for the excited state [55]. By solving the continuity equations (8) and the transmission line equations (16) and (17) with the boundary conditions (19), the transient behaviour of the anode current of the laser tube can be obtained.

4. Method of solution

In the previous section we concluded that the system of governing equations is a mixed system of ordinary and partial differential equations, i.e. the continuity equations are a system of ordinary differential equation (8), while the transmission line equations are a system of partial differential equations (16) and (17). Since the Townsend coefficients are dependent on the electric field and the resistance of each medium is a function of the electron concentration, the continuity equations and the network equations are coupled. There are many numerical methods for solution of the system of partial differential equations (16) and (17) [56–68]. In order to convert the transmission line system of partial differential equations into a system of ordinary differential equations, the strip line constructed by the dielectric plates is approximated by a lumped non-linear RC circuit as shown in figure 2. The transmission line equations, which are written for a distributed RC circuit, are converted into a system of ordinary differential equations for a lumped non-linear RC circuit.

Table 1. Erorr function values (e_1) for some values of dielectric plates division (N).

N	10	15	20	25	30	35	40
$e_1^{(N)}$	35×10^{-2}	46×10^{-4}	29×10^{-5}	52×10^{-6}	93×10^{-7}	12×10^{-7}	41×10^{-8}

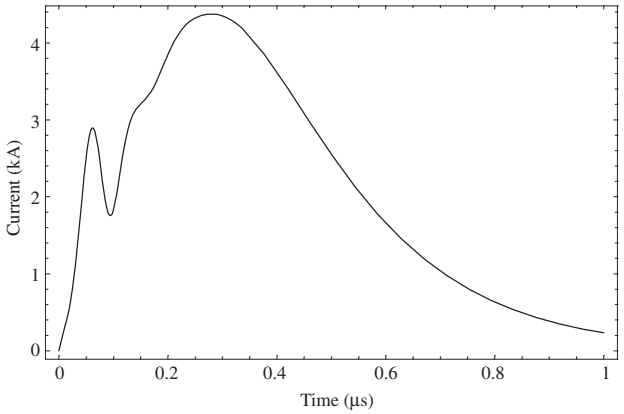

Figure 3. The anode current versus time for a TEA CO_2 laser; the Marx generator voltage is 95 kV and the gas mixture is $CO_2 : N_2 : He = 1 : 1 : 8$.

For the equivalent circuit (figure 2), the Kirchhoff current law at the nodes V_C, V_A, V_j ($j = 1, \ldots, N-1$) and V_N are written. With some mathematical manipulation, we have:

$$\frac{dV_C}{dt} = -\frac{g+g_1}{C_M}V_A + \frac{g_1}{C_M}V_1, \tag{20}$$

$$\frac{dV_A}{dt} = \frac{1}{L(g+g_1)}V_C - \frac{1/L + dg/dt + dg_1/dt - g_1^2/C_1}{g+g_1}V_A + \frac{dg_1/dt - (g_1/C_1)(g_1+g_2)}{g+g_1}V_1 + \frac{g_1 g_2}{C_1(g+g_1)}V_2, \tag{21}$$

$$\frac{dV_j}{dt} = \frac{g_j}{C_j}V_{j-1} - \frac{g_j+g_{j+1}}{C_j}V_j + \frac{g_{j+1}}{C_j}V_{j+1}, \quad j = 1, \ldots, N-1, \tag{22}$$

$$\frac{dV_N}{dt} = \frac{g_N}{C_N}V_{N-1} - \frac{g_N}{C_N}V_N - \frac{I_S}{C_N}, \tag{23}$$

where $g(1/R)$ is the conductance of the plasma between the anode and the cathode electrodes in the main discharge region, $g_j(1/R_j)$ is the conductance of the plasma channel between the $(j-1)$th and jth divisions on the dielectric plates, V_j is the voltage of the jth division on the dielectric plates, V_A is the voltage of the anode, V_C is the voltage of the main capacitor relative to the cathode, C_j is the capacitance of the jth portion of the dielectric plates and L is the inductance of the ignition and the transmission line of the laser system. It should be noted that the inductance of the laser tube and the resistance of the transmission line and resistance of the ignition system are neglected. Generally, for non-uniform divisions on the dielectric plates or for non-uniform thickness dielectric plates, the C_j values are unequal. In this work, it is assumed that the capacitance per unit width (C) is constant over the dielectric plates [65–68] and the widths of the dielectric plates are divided uniformly; hence, in our calculations, C_j is constant over j. The conductances g and g_j are related to the electron concentration by equation (7).

Table 2. Parameter values.

Symbol	Quantity	Values
d	Electrode separation distance	2 (cm)
b	Distance between the dielectric plates	3.85 (cm)
μ_e	Electron mobility	3427 ($cm^2\ V^{-1}\ s^{-1}$)
l	Length of the laser tube	60 (cm)
k	Relative permittivity	7
w	Dielectric thickness	0.4 (cm)
L	Self-inductance of the driving circuit	200 (nH)
C_M	Main capacitance	360 (nF)
β	Recombination rate coefficient	10^{-7} ($cm^3\ s^{-1}$)
N_0	Background gas density	2.45×10^{19} (cm^{-3})
κ_0	Absorption coefficient of a central photon at the resonance frequency	10^{-6} (cm^{-1})
τ	Lifetime of the excited states	10^{-8} (s)
γ_p	Secondary electron emission coefficient due to photon impact	10^{-3}
c	Light velocity	3×10^{10} ($cm\ s^{-1}$)
h	Planck's constant	6.6253×10^{-34} (J s)
A_{r0}	Transition probability for the resonance transition	6.8×10^7 (s^{-1})
ζ	Electrical energy to the radiation energy conversion efficiency	0.1
A	Constant	$3.011\,37 \times 10^{-3}$
B	Constant	84.6956×10^{-3}

In addition to the above equations the electron continuity equation is written for each of the plasma channels between two adjacent sections on the dielectric plate, and it is also written for the plasma in the main discharge region:

$$\frac{dn_{ej}}{dt} = S_j + \alpha_j |V_j| n_{ej} - \beta n_{ej}^2, \qquad j = 0, 1, \ldots, N, \tag{24}$$

where n_{e0} is the electron concentration in the main discharge region and n_{ej} ($j = 1, \ldots, N$) is the electron concentration in the plasma channels on the dielectric plates. The Townsend ionization coefficients are determined by the following relations [36]:

$$\frac{\alpha_j(E_j/N_0)}{p} = 2 \cdot 13 \times 10^9 \exp\left(-100\left|\frac{E_j}{N_0}\right|^{0.57}\right), \quad j = 0, 1, \ldots, N\ (cm^{-1}\,atm^{-1}), \tag{25}$$

where α_j (cm^{-1}) is the Townsend ionization coefficient, p (atm) is the pressure of the laser medium, N_0 (cm^{-3}) is the molecule concentration and E_j ($V\,cm^{-1}$) is the electric field and is derived from the following relations:

$$E_j = \sqrt{N\left(\frac{V_{j+1} - V_{j-1}}{2d}\right)^2 + \left(k\frac{V_j}{w}\right)^2}, \quad j = 1, \ldots, N \tag{26}$$

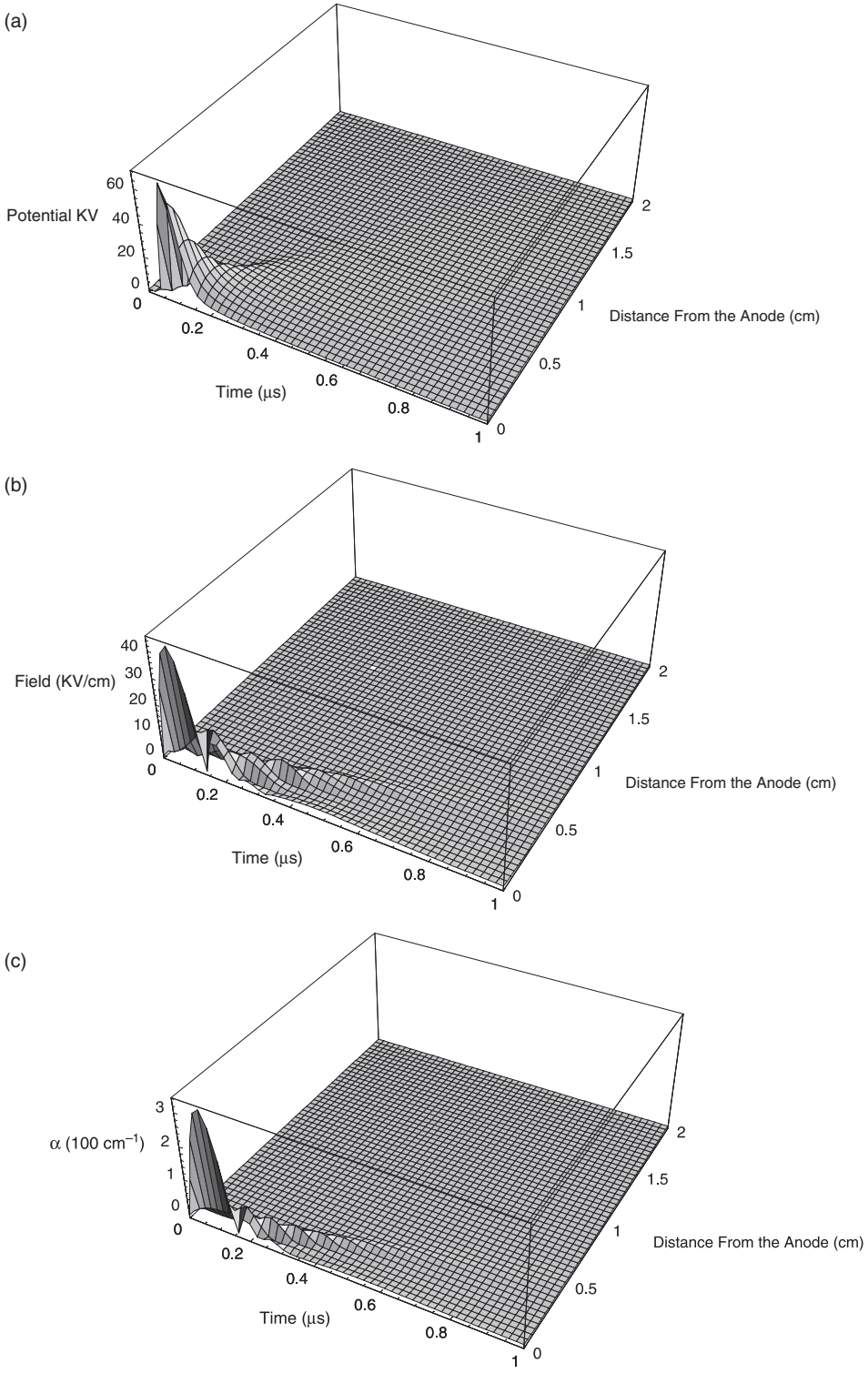

Figure 4. Some physical parameters along the width of the dielectric plates as functions of time: (*a*) electric potential along the width of the dielectric plates, (*b*) electric field along the width of the dielectric plates, (*c*) Townsend first ionization coefficient (α) along the width of the dielectric plates versus time; the Marx generator voltage is 95 kV and the gas mixture is $CO_2 : N_2 : He = 1 : 1 : 8$.

and

$$E_0 = \frac{V_A}{d} \qquad \text{for } j = 0. \tag{27}$$

Let the state variable vector $X_N^T = (V_C, V_A, V_1, \ldots, V_N, n_{e0}, \ldots, n_{eN})$ and the right-hand side of equations (20)–(24) be denoted by $F(X_N)$; then, the state variable equations are written in the standard form:

$$\frac{dX_N}{dt} = F(X_N). \tag{28}$$

For N-sections on the dielectric plates $X_N \in \Re^{2N+3}$, $F : \Re^{2N+3} \to \Re^{2N+3}$ instead of a mixed system of non-linear

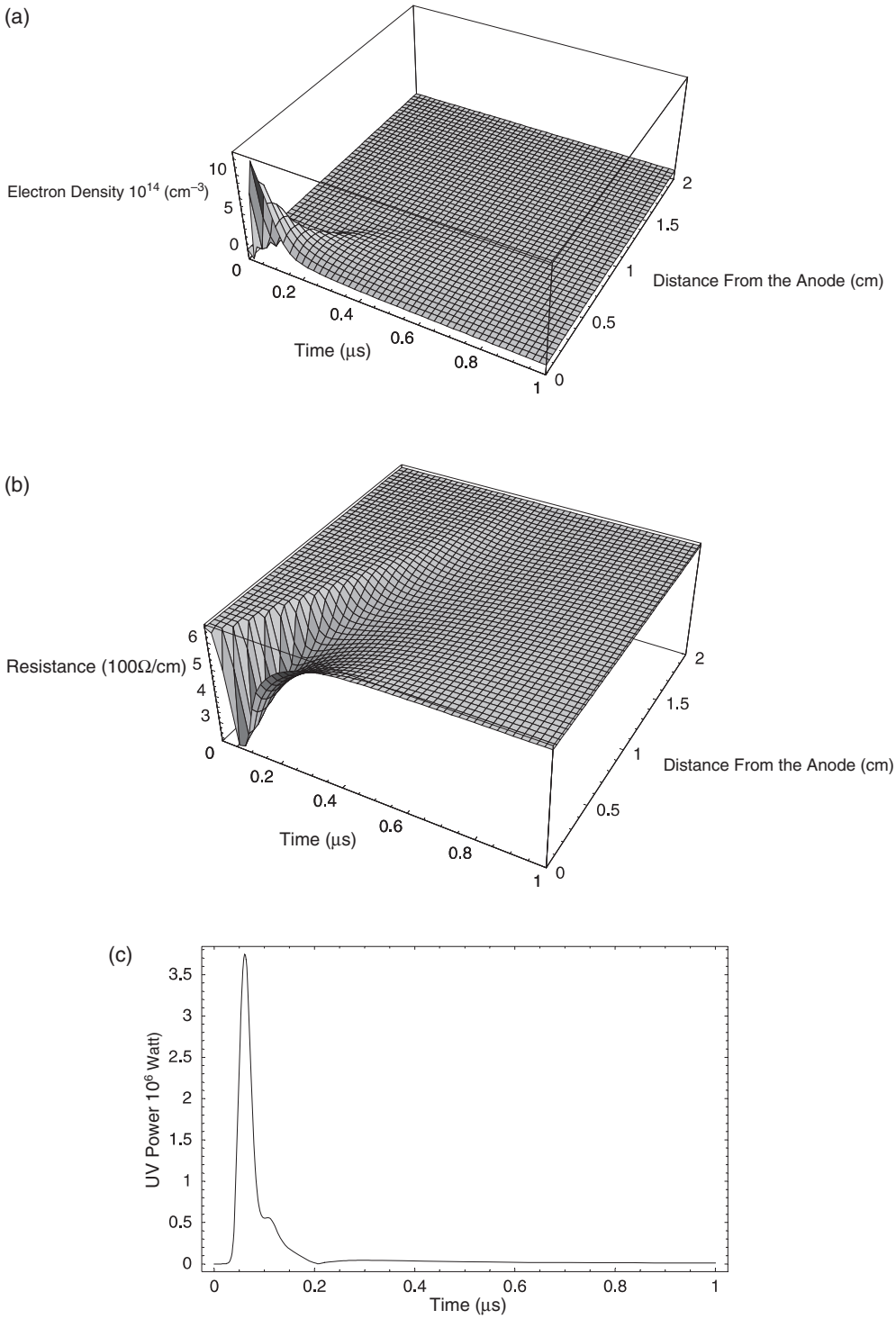

Figure 5. Some physical parameters of the plasma column on the dielectric plates: (*a*) density of free electrons along the width of dielectric plates versus time, (*b*) resistance per unit length of the plasma column along the width of the dielectric plates versus time, (*c*) radiated power in the ultraviolet region by the plasma column on the dielectric plates versus time; the Marx generator voltage is 95 kV and the gas mixture is $CO_2 : N_2 : He = 1 : 1 : 8$.

partial and ordinary differential equations, a system of ordinary differential equations is now obtained.

The system of ordinary non-linear differential equation (28) is solved by the fourth order Runge–Kutta numerical method.

In the lumped circuit model, the number of governing differential equations ($N_{eq} = 2N + 3$) is determined by the number of divisions on the dielectric plates. The error function (e_1) for numerical calculations is given by:

$$e_1^{(N)} = \frac{\int_0^\infty (i_A(t, N) - i_A(t, N-1))^2 \, dt}{\int_0^\infty i_A^2(t, N) \, dt}, \tag{29}$$

where $i_A(t, N-1)$ and $i_A(t, N)$ are the anode currents for $(N-1)$ and N divisions on the dielectric plates, respectively.

This means that the results of the N-divisions on dielectric plates model is compared with the results of the $(N-1)$ divisions model. If the error is acceptable, the problem is solved and if not, the solution of the $(N+1)$th division problem is obtained and so on.

The speed of convergence of the numerical solution of the system of ordinary differential equation (28) is shown in the table 1. In table 1, values of $e_1^{(N)}$ for some N values are compared. As shown in table 1 the speed of convergence of the numerical process is very fast. For an error less than 1%, 13 divisions on the dielectric plates is enough. The calculated anode current versus time is presented in figure 3, which is in good agreement with the Ernst experimental published data [11–14].

5. Results and discussion

The purpose of this study was to focus on the electrical transient behaviour of a TEA CO_2 laser with dielectric corona pre-ionization. As mentioned in the previous sections the transient behaviour of the anode pulse current versus time is determined by (i) the separation distance between the electrodes, (ii) the main discharge capacitance, (iii) the discharge voltage, (iv) the gas pressure in the discharge region and (v) the gas mixture. The distance between electrodes is 2 cm and the parameter values used for calculation are shown in table 2. Unless noted otherwise, the conditions were at their base value (table 2).

The transient voltage, electric field and Townsend ionization coefficient on the dielectric surfaces are shown in figure 4. As expected, the electric field and ionization coefficient near the anode electrode are extremely high and decreasing rapidly towards the cathode surface.

Figure 5 shows the electron concentration on the dielectric plates, plasma surface resistance per unit width and the radiated UV intensity by surface plasma versus time. With the arrival of a voltage pulse at the anode, a sharply inhomogeneous electric field having a large normal component is presented. The ensuing impact ionization of gas near the surface of the dielectric produces a weak pre-discharge streamer travelling along the surface towards the anode. Upon completion of the discharge circuit, the current flow in the conducting channel produces a plasma column just above the surfaces.

The UV photons radiated by the plasma column produce photo-electrons in the main discharge region and the resistance of the main discharge region decreases rapidly. Figure 6 shows the resistance of the main discharge region and electron concentration in the laser active medium. As shown in figure 1(*b*) and seen in Ernst experimental observations, the surface capacitance charges before the first maximum value of the anode current and when the electron concentration in the laser active medium reaches its maximum value the second maximum of the anode current occurs.

The results of this theoretical study are in agreement with the Ernst experimental observations. The UV energy per pulse

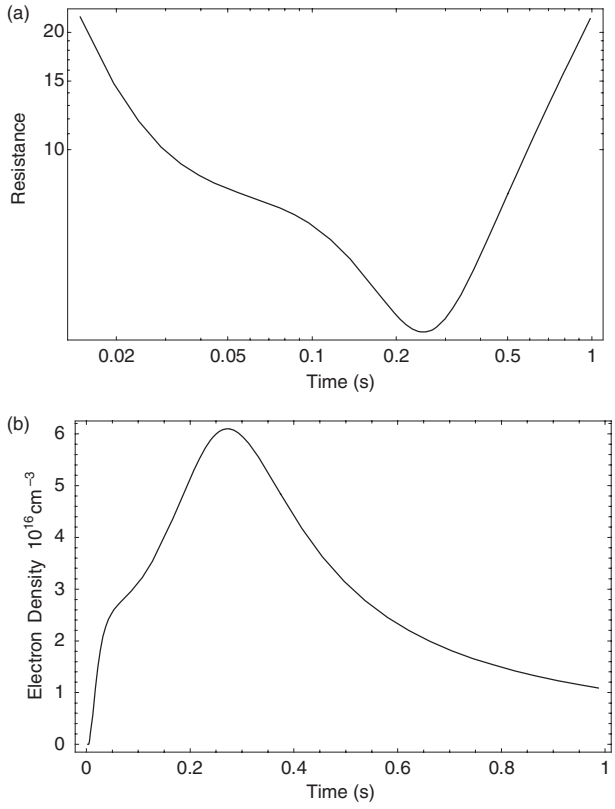

Figure 6. Some physical parameters of the plasma in the main discharge region of the laser tube: (*a*) resistance of the plasma column in the main discharge region as a function of time, (*b*) concentration of free electrons in the main discharge region versus time; the Marx generator voltage is 95 kV and the gas mixture is $CO_2 : N_2 : He = 1 : 1 : 8$.

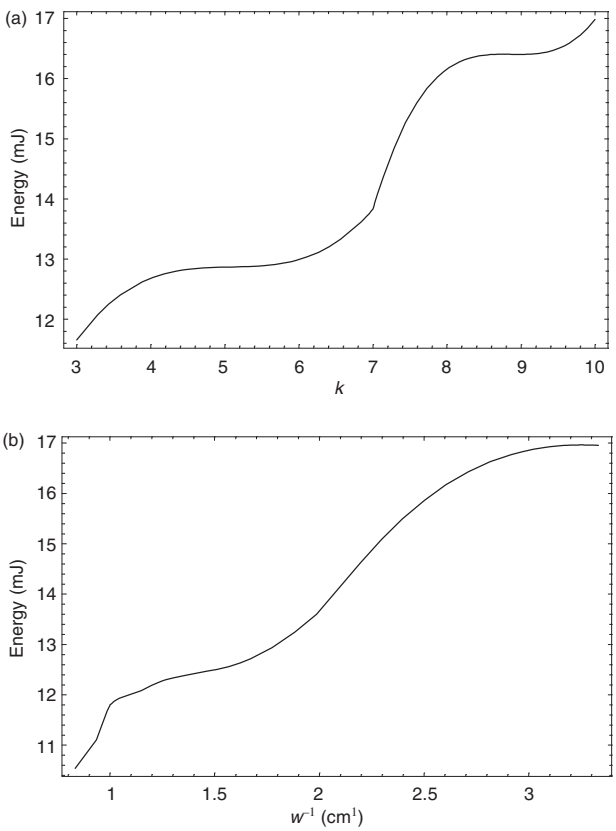

Figure 7. Energy radiated by the plasma column on the dielectric surfaces in the ultraviolet region per pulses: (*a*) versus the dielectric permittivity (k), (*b*) versus the inverse of the dielectric thickness (w^{-1}); the Marx generator voltage is 95 kV and the gas mixture is $CO_2 : N_2 : He = 1 : 1 : 8$.

versus the dielectric relative permittivity (k) and the inverse of the dielectric plates thickness (w^{-1}) are shown in figure 7. Since the calculations are based on equilibrium models, the spark breakdown on the dielectric surfaces is not predictable by this theory. As expected, as a result of the increases in the dielectric relative permittivity or decreases in the thickness of the dielectric plates, the normal component of the electric field increases. This means that if we forget the spark breakdown effects on the dielectric plates, the energy of the UV pulses are increasing functions versus the dielectric relative permittivity and the inverse of the dielectric thickness. Beverly shows that the initial rate of energy input in the surface discharge channel and also its light emission are largely dependent on the initial rate of current change with time [21]. The initial rate of change of current is proportional to the applied voltage and it is also proportional to the inverse of the inductance of the driving circuit. A rapid change of current requires a low inductance of the circuit. Since in this model the effects of surface evaporization due to the strong discharge region are neglected, no limitation is applied to the lower limit of the inductance of the driving circuit. Figure 8(a) shows the UV energy per pulse versus the equivalent inductance of the driving circuit and the results are in good agreement with the experimental and theoretical results presented by Beverly [21, 48]. In figure 8(b) the UV energy per pulse versus the gas pressure is presented. The UV energy produced by the dielectric surfaces for a constant voltage decreases as pressure increases because at a constant voltage with increasing pressure the rate of current change decreases. As stated before, the rate of current change with time determines largely the light emission energy. The greater the rate of change of current with time, the more intense is the light emission. The UV energy per pulse is calculated for different electrode distances and the results are presented in figure 8(c). As expected for a constant voltage and dielectric thickness, the UV radiation energy decreases as the electrode distance increases.

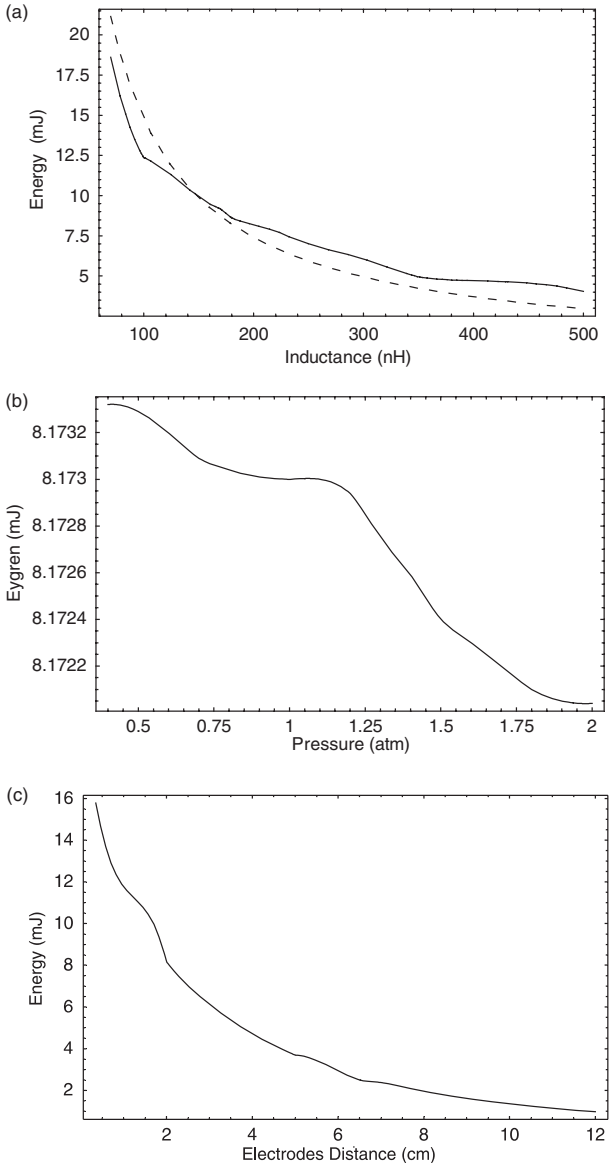

Figure 8. Energy radiated by the plasma column on the dielectric surfaces in the ultraviolet region per pulses: (a) versus the equivalent inductance of the driving circuit. The dashed and solid curves correspond to the Beverly approximation and our calculations, respectively, (b) versus the gas pressure, (c) versus the electrode distance; the Marx generator voltage is 95 kV and the gas mixture is $CO_2 : N_2 : He = 1 : 1 : 8$.

6. Conclusions

As a result of this theoretical analysis we arrived at an explanation of the transient behaviour of the anode current pulse in a TEA CO_2 laser with dielectric corona pre-ionization. In this equilibrium model, the discharge tube of the laser is modelled by a non-linear RC electric circuit. In this model the effect of external circuit is also considered. By this model, the effects of the dielectric relative permittivity, dielectric thickness and pressure of gas in the laser active medium on the laser anode current are obtained. Moreover, it is clear that closer agreement between theory and experiment is possible and work is proceeding towards this end. In our opinion the dominant processes should be included in the theory; however, further considerations need to take into account the effects of non-equilibrium, detachment, stochastic delay, formation delay and meta-stable atoms in the model.

References

[1] Dumanchin B, Michon M, Farcy J C, Boudinet G and Rocca-Serra J 1972 *IEEE J. Quantum Electron.* **QE-8** 163–5
[2] Kumar M and Nath A K 1994 *Opt. Engng.* **33** 1885–8
[3] Suzuki S, Ishibashi Y, Obara M and Fujioka T 1980 *Appl. Phys. Lett.* **36** 26–8
[4] Seguin H J, Tulip J and Mcken D C 1974 *IEEE J. Quantum Electron.* **QE-17** 311–19
[5] Babcock R V, Liberman I and Partlow W D 1976 *IEEE J. Quantum Electron.* **QE-12** 29–34
[6] Scott S J and Smith L S 1988 *J. Appl. Phys.* **64** 528–36
[7] Yamabe C, Matsushita T, Sato S and Horii K 1980 *J. Appl. Phys.* **51**
[8] Witteman W J 1987 *The CO_2 Laser* vol 53 (New York: Springer)
[9] Evans J M 1990 *Selected Paper on CO_2 Laser* vol MS-22 (Bellingham, WA: SPIE Optical Engineering Press)
[10] Eden J G 1999 *Selected Paper on Gas Laser Technology* vol MS-159 (Bellingham, WA: Optical Engineering Press)
[11] Ernst G J and Boer A G 1980 *Opt. Commun.* **34** 221–2

[12] Ernst G J and Boer A G 1978 *Opt. Commun.* **27** 105–10
[13] Ernst G J 1982 *Opt. Commun.* **44** 125–9
[14] Ernst G J 1984 *Opt. Commun.* **49** 275–7
[15] Kushner M J, Pindroh A L, Fisher C H, Znotis T A and Ewing J J 1985 *J. Appl. Phys.* **57** 2406–23
[16] Dhali S K 1989 *IEEE Trans. Plasma Sci.* **17** 603–11
[17] Dadelszen M V and Rote D E 1991 *IEEE Trans. Plasma Sci.* **19** 329–39
[18] Wiener M 2001 *Electromagnetic Analysis Using Transmission Line Variables* (London: World Scientific)
[19] Midorikawa K, Obara M and Fujioka T 1984 *IEEE J. Quantum Electron.* **QE-20** 198–205
[20] Raizer Y P 1991 *Gas Discharge Physics* (New York: Springer)
[21] Beverly R E 1978 *Light Emission From High-Current Surface-Spark Discharges* vol 16 (North Holland, Amsterdam: Progress Optics)
[22] Levatter J I and Lin S 1980 *J. Appl. Phys.* **51** 210–22
[23] Kushner M J 1991 *IEEE Trans. Plasma Sci.* **19** 387–99
[24] Persephonis P, Giannetas V, Georgiades C, Parthenios J and Ioannou A 1995 *IEEE J. Quantum Electron.* **31** 573–81
[25] Persephonis P, Giannetas V, Georgiades C, Parthenios J and Ioannou A 1995 *IEEE J. Quantum Electron.* **31** 567–72
[26] Persephonis P 1987 *J. Appl. Phys.* **62** 2651–6
[27] Papadopoulos A D and Serafetinides A A 1990 *IEEE J. Quantum Electron.* **26** 177–88
[28] Persephonis P, Vlachos K, Georgiades C and Parthenios J 1992 *J. Appl. Phys.* **71** 4755–62
[29] Morrow R and Sato N 1999 *J. Phys. D: Appl. Phys.* **32** L20–2
[30] Morrow R 1985 *Phys. Rev.* A **32** 3821–4
[31] Coutts J and Webb C E 1986 *J. Appl. Phys.* **59** 704–10
[32] Graves D B and Jensen K F 1986 *IEEE Trans. Plasma Sci.* **PS-14** 78–91
[33] Bletzinger P and Ganguly B N 2003 *J. Phys. D: Appl. Phys.* **36** 1550–2
[34] Revel I, Belenguer P, Bœuf J P and Pitchford L C 1999 *Pure Appl. Chem.* **71** 1837–44
[35] Lowke J J, Phelps A V and Irwin B W 1973 *J. Appl. Phys.* **44** 4664–8
[36] Young F F and Wu J 1993 *J. Phys. D: Appl. Phys.* **26** 782–92
[37] Guo J and Wu J 1993 *IEEE Trans. Plasma Sci.* **21** 684–95
[38] Meek J M and Cragge J D 1976 *Electrical Breakdown of Gases* (Oxford: Clarendon)
[39] Phelps A V 1960 *Phys. Rev.* **117**
[40] Lozanskii E D and Firsov O B 1969 *Sov. Phys. JETP* **29** 367–9
[41] Lozanskii E D and Firsov O B 1973 *J. Phys. D: Appl. Phys.* **6** 976–81
[42] Holstein T 1947 *Phys. Rev.* **72** 1212–33
[43] Holstein T 1951 *Phys. Rev.* **83** 1159–68
[44] Lozanskii E D 1976 *Sov. Phys.—Usp.* **18** 493–521
[45] Lozanskii E D and Pontekorvo D B 1975 *Sov. Phys. Tech. Phys.* **19** 1432–3
[46] Lozanskii E D 1969 *Sov. Phys. Tech. Phys.* **13** 1269–72
[47] Lozanskii E D and Firsov O B 1973 *J. Phys. D: Appl. Phys.* **6** 976–81
[48] Beverly R E 1986 *J. Appl. Phys.* **60** 104–24
[49] Beverly R E 1991 *J. Appl. Phys.* **69** 3830–4
[50] Beverly R E 1988 *J. Appl. Phys.* **64** 1753–7
[51] Beverly R E 1986 *J. Appl. Phys. Lett.* **58** 1024–6
[52] Seguin H J J, Mcken D and Tulip J 1976 *J. Appl. Phys. Lett.* **28** 487–9
[53] Basov N G 1975 *Pulse Gas-Discharge Atomic and Molecular Laser* (New York: Consultants Bureau)
[54] Raether H 1964 *Electron Avalanche and Breakdown In Gases* (London: Butterworths)
[55] Georghiou G E, Morrow R and Metaxas A C 2000 *J. Phys. D: Appl. Phys.* **33** L27–32
[56] Kline L E 1974 *J. Appl. Phys.* **45** 2046–54
[57] Dhali S K and Williams P F 1985 *Phys. Rev.* A **31** 1219–21
[58] Choi K C and Whang K 1995 *IEEE Trans. Plasma Sci.* **23** 399–404
[59] Lymberopoulos D P and Economou D J 1993 *J. Appl. Phys.* **73** 3668–79
[60] Boeuf J P 1987 *Phys. Rev.* A **36** 2782–92
[61] Schmitt W, Kohler W E and Ruder H 1992 *J. Appl. Phys.* **71** 5783–91
[62] Hitchon W N G, Parker G J and Lawler J E 1993 *IEEE Trans. Plasma Sci.* **21** 228–38
[63] Kline L E and Siambis J G 1972 *Phys. Rev.* A **5** 794–805
[64] Davies A J, Davies C S and Evans C J 1971 *Proc. IEE* **118** 816–23
[65] Kadish A, Robiscoe R T and Maier W B 1989 *J. Appl. Phys.* **66** 1579–93
[66] Robiscoe R T and Kadish A 1991 *IEEE Trans. Plasma Sci.* **19** 529–34
[67] Kadish A and Robiscoe R T 1989 *J. Appl. Phys.* **66** 4123–33
[68] Kadish A, Maier W B and Robiscoe R T 1991 *IEEE Trans. Plasma Sci.* **19** 697–704